

## Optical Study of the $\text{Sr}_{14-x}\text{Ca}_x\text{Cu}_{24}\text{O}_{41}$ System: Evidence for Hole-Doped $\text{Cu}_2\text{O}_3$ Ladders

T. Osafune, N. Motoyama, H. Eisaki, and S. Uchida

*Department of Superconductivity, The University of Tokyo, Bunkyo-ku, Tokyo 113, Japan*

(Received 15 October 1996)

The optical conductivity spectrum of  $\text{Sr}_{14-x}\text{Ca}_x\text{Cu}_{24}\text{O}_{41}$ , composed of two-leg  $\text{Cu}_2\text{O}_3$  ladders and edge-sharing  $\text{CuO}_2$  chains, is investigated on single crystals with various compositions. Upon isovalent Ca substitution for Sr a rapid transfer of the spectral weight takes place from the high- to low-energy region, essentially in the same manner as that observed in the doped  $\text{CuO}_2$  planes of high- $T_c$  cuprates. We identify this behavior as a consequence of charge redistribution between chains and ladders, and estimate the hole density in each structural unit from the transferred spectral weight. [S0031-9007(97)02577-5]

PACS numbers: 74.72.Jt, 78.20.-e, 78.30.-j

Recent theoretical predictions [1] have attracted much attention to the antiferromagnetic  $S = \frac{1}{2}$  two-leg ladder system. It is predicted that the even-leg ladders have a spin liquid ground state with a spin gap [2] and that doping into the spin ladders results in the pairing of the doped holes which leads to the formation of bipolarons or superconducting Cooper pairs [3]. Such predictions have been extensively tested and the spin gap has been observed in real materials, such as  $(\text{VO})_2\text{P}_2\text{O}_7$  [4], or  $\text{SrCu}_2\text{O}_3$  [5]. Furthermore, the recent report of a superconductivity signal in  $\text{Sr}_{0.4}\text{Ca}_{13.6}\text{Cu}_{24}\text{O}_{41}$  by Uehara *et al.* [6] under a pressure of 3GPa is expected to be a manifestation of the latter prediction.

$\text{Sr}_{14-x}\text{Ca}_x\text{Cu}_{24}\text{O}_{41}$  is composed of the alternating stacks of the plane of the edge sharing  $\text{CuO}_2$  chain, (Sr, Ca) layer, and the plane including the two-leg  $\text{Cu}_2\text{O}_3$  ladder [7]. The nominal valence of Cu is +2.25, independent of  $x$ , so the system is inherently doped with holes. In spite of its high Cu valence,  $\text{Sr}_{14}\text{Cu}_{24}\text{O}_{41}$  shows semiconducting behaviors. Magnetically, a gap is observed in the spin excitations of both chains and ladders [8–10]. With increasing Ca content substituted for Sr (or with increasing applied pressure), the resistivity remarkably decreases [11,12]. As the Ca substitution does not change the average valence of Cu, it is speculated that the localized holes become mobile due to the increased overlap of the Cu  $3d$  and O  $2p$  wave functions [12] or that redistribution of the hole density from immobile sites takes place considering the existence of two possible paths in this system [11]. To understand the properties of this system, one has to know how the holes are distributed between chains and ladders.

In this paper, the quantitative analysis of the evolution in the optical conductivity induced by Ca substitution makes it possible to isolate the contribution from ladders and chains, respectively. The low-energy excitations are ascribable to the ladders on which holes are much more itinerant than on the chains. From the conductivity sum-rule we estimate the hole density in each unit and show

that the holes are transferred from chains to ladders upon Ca substitution.

Single-crystalline samples of  $\text{Sr}_{14-x}\text{Ca}_x\text{Cu}_{24}\text{O}_{41}$  up to  $x = 11$  were grown by the traveling-solvent floating zone (TSFZ) method. The  $x = 11$  sample shows a metallic resistivity along the  $c$  axis ( $\rho_c$ ) down to 80 K, below which the resistivity shows insulating behavior. Other compounds with lower Ca content are semiconducting over the entire temperature range below 300 K. The results of the magnetic susceptibility and electrical resistivity measurements are reported previously in another paper [13]. Reflectivity was measured at room temperature using polarized light in the energy range 0.01–40 eV at near-normal incidence to the  $a$ - $c$  plane (the ladder plane with  $c$  axis parallel to ladders).

Figure 1 shows the reflectivity spectra of  $\text{Sr}_{14-x}/\text{A}_x\text{Cu}_{24}\text{O}_{41}$  with the polarization parallel to the  $c$  axis.  $\text{Sr}_{14}\text{Cu}_{24}\text{O}_{41}$  shows a plasma edge at  $\sim 0.5$  eV. Apparently that contradicts the semiconducting temperature dependence of resistivity with an activation energy of about 2200 K. However, it turns out that  $\text{Sr}_{14}\text{Cu}_{24}\text{O}_{41}$  is not a genuine insulator, since the Y-substituted compounds  $\text{Sr}_{14-x}\text{Y}_x\text{Cu}_{24}\text{O}_{41}$  have higher resistivities with a larger activation energy [13]. The Y substitution nominally reduces the hole density in both ladders and chains. In fact, for the Y-substituted material, the plasma edge disappears and the spectrum is dominated by the optical phonons (see inset) and the interband gap excitations are clearly observed at  $\sim 2$  eV. Thus, it is concluded that there is a small but finite density of carriers in  $\text{Sr}_{14}\text{Cu}_{24}\text{O}_{41}$ . The carriers would be easily localized due to disorder in this one-dimensional (1D) system as this material. Since the localization is a low-energy phenomenon, the material recovers metallic features at optical frequencies, giving rise to a plasma edge in the reflectivity spectrum. In contrast to the Y substitution, the plasma edge shifts towards higher energies with increasing Ca substitution. Both the shape of the reflectivity spectrum and the position of the reflectivity edge are essentially similar

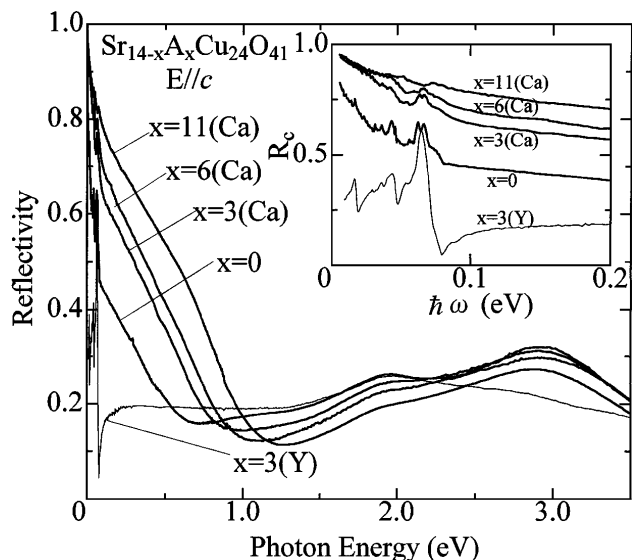


FIG. 1. Reflectivity spectra below 3.5 eV for various compositions of  $\text{Sr}_{14-x}\text{A}_x\text{Cu}_{24}\text{O}_{41}$  measured at room temperature with polarization  $E||c$ . The low-energy spectra below 0.2 eV are shown in the inset.

to those of the two-dimensional (2D) cuprates such as  $\text{La}_{2-x}\text{Sr}_x\text{CuO}_4$  [14]. However, such a large shift in the plasma edge is not observed in the 2D case.

For quantitative discussions, the Kramers-Kronig transformation is made on the reflectivity spectrum. In Fig. 2, we show the evolution of the optical conductivity spectrum with Ca content  $x$  for polarization  $E||c$ . The optical conductivity spectrum of  $\text{Sr}_{11}\text{Y}_3\text{Cu}_{24}\text{O}_{41}$  is typical of insulators. The spectrum is characterized by a peak at 2.0 eV. The most possible origin for the peak is the charge-transfer (CT) excitation between Cu 3d and O 2p states which is commonly observed in the parent insulators of high- $T_c$  cuprates. On moving to  $\text{Sr}_{14}\text{Cu}_{24}\text{O}_{41}$  and further  $\text{Sr}_{14-x}\text{Ca}_x\text{Cu}_{24}\text{O}_{41}$ , the conductivity in the low-energy region (below 1.2 eV) increases, whereas the CT spectral weight decreases.

It turns out from the sum-rule analysis described below that the CT spectral weight (SW) is transferred only to the low-energy excitations below 1.2 eV. Such SW transfer is essentially the same as that seen in the 2D cuprates when a parent CT insulator is doped with carriers [14]. Then, it follows that carriers, certainly holes, are doped into a structural unit, which is a CT insulator in  $\text{Sr}_{11}\text{Y}_3\text{Cu}_{24}\text{O}_{41}$  with a CT energy gap of  $\sim 2$  eV and that the doped hole density increases with Ca content. As the substitution of isovalent Ca does not change the average Cu valence in the system, a redistribution of holes between chains and ladders should be induced by the Ca substitution. Therefore, the shift of the plasma edge shown in Fig. 1 is a consequence of increased carrier density, not a consequence that the originally localized carriers become itinerant with Ca substitution. Theoretically, the spectral weight transfer is a general

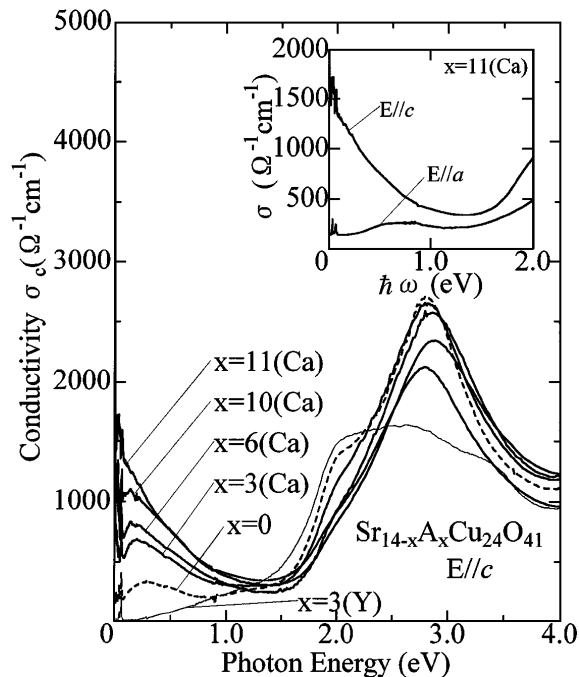


FIG. 2.  $c$ -axis optical conductivity spectrum  $\sigma_c(\omega)$  obtained from the Kramers-Kronig transformation of the reflectivity spectra for various compositions of  $\text{Sr}_{14-x}\text{A}_x\text{Cu}_{24}\text{O}_{41}$ . The anisotropic spectra with  $a$ - and  $c$ -axis polarization are shown for  $\text{Sr}_3\text{Ca}_{11}\text{Cu}_{24}\text{O}_{41}$  in the inset.

feature induced by carrier doping into a Mott or CT insulator, irrespective of its dimensionality [15,16].

Based on the conductivity data, we estimate the spectral weight in terms of the effective electron number;

$$N_{\text{eff}}(\omega) = \frac{2m_0V}{\pi e^2} \int_0^\omega \sigma_c(\omega') d\omega',$$

where  $m_0$  is taken as the free electron mass, and  $V$  is the volume containing one Cu atom.  $N_{\text{eff}}(\omega)$  is proportional to the number of electrons involved in the optical excitations up to  $\hbar\omega$ . In Fig. 3 we plot the result of  $N_{\text{eff}}(\omega)$ . It is important that  $N_{\text{eff}}$  is not strongly dependent on  $x$  at  $\hbar\omega \sim 2.5$  eV. This provides evidence that the SW transfer is taking place within the energy range below  $\sim 2.5$  eV and thus most of the CT spectral weight is transferred to the low-energy region.

Another point in Fig. 3 is the magnitude of  $N_{\text{eff}}$ .  $N_{\text{eff}}$  at 1.2 eV represents the spectral weight of the low-energy excitations transferred from the high-energy CT excitation with "doping" which is a consequence of charge transfer between chains and ladders. Note that the values of  $N_{\text{eff}}(1.2 \text{ eV})$  for the "doped" materials are comparable to those ( $N_{\text{eff}}^{2D}$ ) for the 2D high- $T_c$  cuprates near optimal doping [14]. When the value of  $N_{\text{eff}}$  per Cu is converted into the value per ladder Cu,  $N_{\text{eff}}^L = N_{\text{eff}} \cdot 24/14$ ,  $N_{\text{eff}}^L$  is even larger than  $N_{\text{eff}}^{2D}$  [14]. According to the theoretical calculations based on the Hubbard or  $t$ - $J$  model [15] the low-energy SW is the order of the Cu 3d-O 2p transfer integral  $t$ . In the present system,  $t$  in the  $\text{Cu}_2\text{O}_3$  ladder

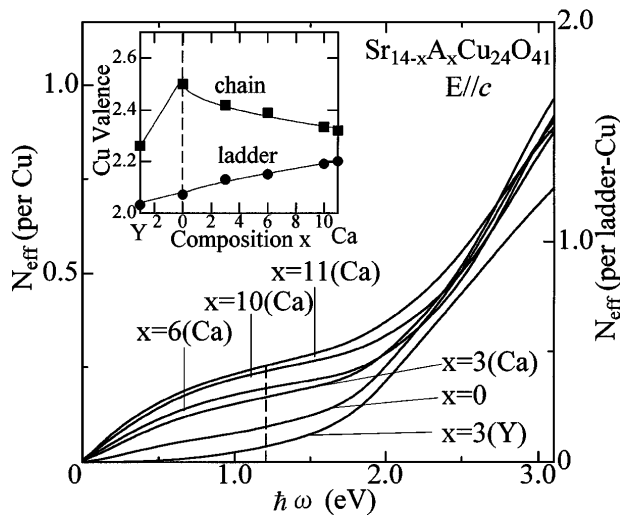


FIG. 3. Effective electron number  $N_{\text{eff}}$  per Cu (left-hand scale) from a conductivity sum is plotted as a function of energy for various compositions.  $N_{\text{eff}}$  per ladder Cu is indicated on the right-hand scale. The valences of both chain- and ladder-Cu estimated from  $N_{\text{eff}}^L$  (1.2 eV) for each composition are plotted in the inset.

is nearly identical to that in the  $\text{CuO}_2$  planes of the high- $T_c$  cuprates since the corner-sharing  $\text{CuO}_4$  network with  $180^\circ$  Cu-O-Cu bonds is common between the two systems. On the other hand,  $t$  in the  $\text{CuO}_2$  chains with  $90^\circ$  Cu-O-Cu bonds should be considerably smaller than  $t$  in the ladders. Therefore, it is reasonable to assign the low-energy excitations to those in the ladders. It follows, accordingly, that the holes are transferred from the charge reservoir chains to the ladder conduction paths. From Figs. 2 and 3, it is also concluded that the holes in the chains remain localized and the charge excitations in the chains start up at  $\sim 2.5$  eV or higher, forming a pronounced peak at  $\sim 3$  eV in  $\text{Sr}_{14-x}\text{Ca}_x\text{Cu}_{24}\text{O}_{41}$ .

Using the value of  $N_{\text{eff}}^L$  which well approximates the effective electron number in the ladders we can estimate the hole density in the ladders. To do that, we make two reasonable assumptions. One is that the chain-Cu valence would be  $+2.5$  in  $\text{Sr}_{14}\text{Cu}_{24}\text{O}_{41}$ . This assumption is supported by the recent neutron scattering measurements [17]. The neutron result gives evidence for a dimerized state between  $\text{Cu}^{2+}$  spins separated by two and four times the distance between the nearest-neighbor chain Cu ions. This can be understood assuming the formation of an alternating  $\text{Cu}^{2+}$ - $\text{Cu}^{3+}$  ordered array along the chain. Then, we can estimate the value of the ladder Cu valence as  $+2.07$ , from the average valence of Cu is  $+2.25$ . The second assumption is a linear relationship between  $N_{\text{eff}}^L$  and the doped hole density  $\delta$ ,  $N_{\text{eff}}^L = A\delta$ . This is predicted by the theoretical calculations on the 1D systems [15,18,19] as far as  $\delta$  is not large. The coefficient  $A$  is determined from the value of  $N_{\text{eff}}^L$  for  $\text{Sr}_{14}\text{Cu}_{24}\text{O}_{41}$  with  $\delta = 0.07$ . Based on these assumptions the hole density or the Cu valence in the ladders as well as in the

chains is estimated for each  $x$  as plotted in the inset of Fig. 3. It is found that at  $x = 11$  the ladder Cu valence reaches  $+2.20$ , that is, 0.2 holes per Cu are doped into ladders. This hole number is as much as that in the high- $T_c$  material near optimal doping [20].

As a consequence of the transfer of holes, the chain Cu valence decreases with Ca substitution (it also decreases with Y substitution). Based on the above-mentioned model of the  $\text{CuO}_2$  chain, the decrease in the chain-Cu valence implies a decrease in the number of  $\text{Cu}^{3+}$  ions which are presumably nonmagnetic due to the formation of Zhang-Rice singlet [12,21] or conversely an increase in the number of magnetic  $\text{Cu}^{2+}$  ions. The increase in the magnitude of a Curie term is, in fact, observed in the magnetic susceptibility for both Ca and Y substituted  $\text{Sr}_{14}\text{Cu}_{24}\text{O}_{41}$  [13] and the Curie term exactly follows the  $x$  dependence of the decrease in the chain-Cu valence (from  $+2.5$ ) shown in the inset. It should also be noted that the intensity of the 3 eV peak in  $\sigma_c(\omega)$  shows the same trend. The peak intensity in the spectrum of  $\text{Sr}_{14}\text{Cu}_{24}\text{O}_{41}$  is rapidly reduced with Y substitution, while it gradually decreases when substituted with Ca, which reconfirms that the 3 eV peak is assigned to the excitations in the chains, certainly related to the  $\text{Cu}^{3+}$  ionic state or the (local)  $\text{Cu}^{2+}$ - $\text{Cu}^{3+}$  order.

Coming back to the optical conductivity spectrum, the evolution of the spectrum with doping as well as the low-energy spectral shape is quite similar to those observed for the 2D cuprates [14]. However, there is a remarkable difference between 1D and 2D cuprates. In the 2D cuprates the reflectivity edge does not shift appreciably with doping as illustrated in Fig. 4. In the 2D case, a so-called mid-IR band centered at relatively high energy ( $\sim 0.5$  eV) rapidly develops upon doping. The difference is ascribable to the fact that in the present ladder system the peak or the center of gravity of the "mid-IR" band in  $\sigma_c(\omega)$  is located at considerably lower energy ( $\sim 0.2$  eV) and that the low-energy SW,  $N_{\text{eff}}^L$  at 1.2 eV, continues to increase as doping proceeds, whereas  $N_{\text{eff}}^{2D}$  saturates (or even decrease) at high dopings.

The theoretical calculations predict that for the doped 1D chains [15] or ladders [19] the mid-IR band is much weaker than the Drude band. It turns out from Fig. 4 that the square of the plasma edge frequency  $\omega_p^2$  is roughly proportional to  $\delta$ , i.e., to  $N_{\text{eff}}^L$  (1.2 eV). This is in contrast to 2D cuprates, and might naturally be explained supposing that most of the low-energy SW arises from a single Drude component [22]. Thus, the difference in the reflectivity spectrum appears to reflect the 1D nature of the electronic state of the present doped ladders. In fact, one-dimensionality is evidenced from the resistivity and optical conductivity in the direction perpendicular to the ladders. For  $x = 11$  the resistivity in the  $a$ -axis direction (parallel to the rungs of ladders) is by a factor of 10–40 higher than  $\rho_c$ , and the  $b$ -axis (perpendicular to the ladder planes) resistivity is still higher by two orders

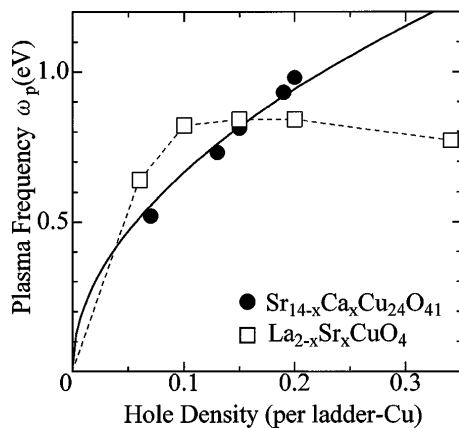


FIG. 4. Plasma-edge energy  $\omega_p$  plotted as a function of the hole density  $\delta$  per ladder Cu and plane Cu ( $\delta = x$ ) for  $\text{Sr}_{14-x}\text{Ca}_x\text{Cu}_{24}\text{O}_{41}$  and  $\text{La}_{2-x}\text{Sr}_x\text{CuO}_4$ , respectively. The plasma-edge energy is determined from the peak position of the loss function ( $\text{Im}[-1/\epsilon(\omega)]$ ). The solid curve following  $\omega_p^2 \sim \delta$  is the best fit to the data of  $\text{Sr}_{14-x}\text{Ca}_x\text{Cu}_{24}\text{O}_{41}$ , and the dashed curve through the data of  $\text{La}_{2-x}\text{Sr}_x\text{CuO}_4$  is a guide for the eyes.

of magnitude than  $\rho_a$  [13]. The optical spectrum for  $E||a$  measured on the same  $x = 11$  sample is shown in the inset of Fig. 2. The magnitude of  $\sigma_a$  is suppressed over a fairly wide energy range and does not form a Drude peak at  $\omega = 0$ . These are reminiscent of the  $c$ -axis (perpendicular to the  $\text{CuO}_2$  planes) resistivity and optical spectrum of the high- $T_c$  cuprates [23].

The slow decay of the low-energy  $\sigma_c(\omega)$ , which approximately follows an  $\omega^{-1}$  dependence, is similar to that observed in the in-plane  $\sigma_{ab}(\omega)$  of optimally doped high- $T_c$  cuprates. This is interpreted either in terms of the two-component model, a Drude plus mid-IR band, or in terms of the one-component model with  $\omega$ -dependent scattering time of the carriers. For doped two-leg ladders, the presence of the weak mid-IR band is theoretically predicted, associated with the dissociation of bipolarons composed of holes on the same rung [19]. In this case the mid-IR band should have a finite threshold energy related to a spin gap and be isolated from a Drude band. However, such a mid-IR band is not clearly identified in the spectrum shown in Fig. 2. Relevance of a spin gap in the ladders which is detected by the NMR measurements [24,25] to the charge dynamics is not clear at present.

In summary, we have studied a systematic evolution of the optical spectrum for single crystals of  $\text{Sr}_{14-x}\text{A}_x\text{Cu}_{24}\text{O}_{41}$  ( $A = \text{Ca}, \text{Y}$ ). The results provide strong evidence that the two-leg  $\text{Cu}_2\text{O}_3$  ladders contained in this system are progressively doped with hole carriers by Ca substitution for Sr as a consequence of charge transfer from the charge reservoir  $\text{CuO}_2$  chains. The holes on the chains are strongly localized and the excitations start up at about 2.5 eV or higher. They obtain itinerancy when transferred onto the ladders. Accordingly, the electronic properties of the present system are determined by the holes doped into ladders, while a

substantial number of holes localized in the chains form a novel magnetic ground state with a spin gap. This picture nicely explains the evolution of the electrical resistivity and magnetic susceptibility with Ca (Y) substitution in  $\text{Sr}_{14}\text{Cu}_{24}\text{O}_{41}$ .

We are grateful to Y. Mizuno, T. Tohyama, and S. Maekawa for helpful discussions. This work is supported by a Grant-in-Aid for Scientific Research from the Ministry of Education, Science, and Culture, Japan, and by NEDO Grants for Advanced Industrial Technology Research and for International Joint Research.

- [1] For a review, see E. Dagotto and T. M. Rice, *Science* **271**, 618 (1996).
- [2] E. Dagotto, J. Riera, and D. J. Scalapino, *Phys. Rev. B* **45**, 5744 (1992).
- [3] H. Tsunetsugu, M. Troyer, and T. M. Rice, *Phys. Rev. B* **51**, 16456 (1995).
- [4] D. C. Johnston *et al.*, *Phys. Rev. B* **35**, 219 (1987).
- [5] M. Azuma *et al.*, *Phys. Rev. Lett.* **73**, 3463 (1994).
- [6] M. Uehara *et al.*, *J. Phys. Soc. Jpn.* **65**, 2764 (1996).
- [7] E. M. McCarron *et al.*, *Mater. Res. Bull.* **23**, 1355 (1988); T. Siegrist *et al.*, *ibid* **23**, 1429 (1988).
- [8] M. Matsuda and K. Katsumata, *Phys. Rev. B* **53**, 12201 (1996).
- [9] R. S. Eccleston, M. Azuma, and M. Takano, *Phys. Rev. B* **53**, R14721 (1996).
- [10] J. Akimitsu *et al.*, *Physica (Amsterdam)* **263C**, 475 (1996).
- [11] M. Kato, K. Shiota, and Y. Koike, *Physica (Amsterdam)* **258C**, 284 (1996).
- [12] S. A. Carter *et al.*, *Phys. Rev. Lett.* **77**, 1378 (1996).
- [13] N. Motoyama *et al.*, *Phys. Rev. B* **55**, 3386 (1997).
- [14] S. Uchida *et al.*, *Phys. Rev. B* **43**, 7942 (1991).
- [15] P. Horsch and W. Stephan, *Phys. Rev. B* **48**, 10595 (1993); H. Eskes *et al.*, *Phys. Rev. B* **50**, 17980 (1994).
- [16] Y. Mizuno, T. Tohyama, and S. Maekawa (unpublished).
- [17] M. Matsuda *et al.*, *Phys. Rev. B* **54**, 12199 (1996).
- [18] M. Imada, *J. Phys. Soc. Jpn.* **64**, 2954 (1995).
- [19] C. A. Hayward, D. Poilblanc, and D. J. Scalapino, *Phys. Rev. B* **53**, R8863 (1996).
- [20] In view of this plot more holes would be doped into ladders in  $\text{Sr}_{0.4}\text{Ca}_{13.6}\text{Cu}_{24}\text{O}_{41}$  which has been reported to exhibit a sign of superconductivity under high pressure [6]. It is speculated that the pressure might have a similar effect to the Ca substitution and further increase the hole density in the ladders beyond a threshold to realize superconductivity. But there may be other possibilities, for example, the high pressure may distort the lattice, making the dimensionality of the electronic state in the ladder higher than one.
- [21] F. C. Zhang and T. M. Rice, *Phys. Rev. B* **37**, 3759 (1988).
- [22] In this regard, the 0.2 eV peak seen in  $\sigma_c(\omega)$  for  $x \leq 6$  may reflect localization of carriers. Actually,  $\rho_c(T)$  exhibits a localization at low temperatures even for the  $x = 11$  sample [13].
- [23] S. Uchida, K. Tamasaku, and S. Tajima, *Phys. Rev. B* **53**, 14558 (1996).
- [24] S. Tsuji *et al.*, *J. Phys. Soc. Jpn.* **65**, 42 (1996).
- [25] S. Matsumoto *et al.* (unpublished).